Pergamon

Int. J. Heat Mass Transfer. Vol. 41, No. 2, pp. 303–311, 1998

Printed in Great Britain
0017–9310/98 $19.00+0.00

PII: S0017–9310(97)00140–3

A dry-spot model of critical heat flux in pool and forced convection boiling

SANG JUN HA and HEE CHEON NO†

Department of Nuclear Engineering, Korea Advanced Institute of Science and Technology, 373-1 Kusong-dong Yusong-gu, Taejon 305-701, Korea

(*Received* 24 *January* 1997 *and in final form* 10 *May* 1997)

Abstract—A new dry-spot model for high heat flux nucleate boiling region and critical heat flux (CHF) is proposed. The new concept of dry area formation based on Poisson distribution of active nucleation sites and the critical active site number is introduced. It is shown that CHF can be determined without any correction factor based on information on the boiling parameters such as active site density and bubble diameter, etc., in the nucleate boiling region. It turns out that the present model well explains the mechanism on how parameters such as flow modes and surface wettability influences CHF. © 1997 Elsevier Science Ltd.

1. INTRODUCTION

The advent of high power systems such as nuclear reactors gave a great impetus to research into critical heat flux (CHF) over the last several decades. The strong interest is due to practical considerations since it is desirable to design a heat exchanger to operate at as high a heat flux as possible with optimum heat transfer rates, yet without risk of physical burnout. Numerous experimental and theoretical studies have been made for a wide variety of boiling conditions, and many correlations of CHF are now available in the literature, with each applicable to somewhat narrow ranges of empirical conditions. However, due to the difficulty in observing detailed flow of the near-wall region at heat fluxes approaching CHF and the sensitivity to the several parameters such as flow modes (pool or flow), the bulk temperature of liquid, the geometry of heating surfaces and surface conditions, many of the published CHF models have been based on postulated mechanisms. A fundamental difference between the various possible approaches to modeling CHF is in how each approach views the process of supply of liquid to the heating surface.

Of the CHF models, the hydrodynamic models including hydrodynamic instability model proposed by Zuber [1] and macrolayer dryout model presented by Haramura and Katto [2] have been most widely accepted. In spite of wide recognition and rather good agreement of the models and experimental results, there are some reasons which make one to doubt the validity of the physical features of the models as pointed out by several researchers [3–5]. Also, if CHF occurs due to hydrodynamic instability only, it is difficult to understand why transition region exists on a boiling curve after heat flux has reached its critical value. The hydrodynamic models exclude any existing influences of the heating surface conditions such as surface wettability effects, thermal properties of the surface material effects on CHF. In connection with parametric effects on CHF, many investigators applied a single model in different boiling conditions in the past, while Dhir [6] stated that different mechanisms dictate CHF with different surface wettability and Sadasivan *et al.* [5] brought forward the possibility that different phenomena might control in different boiling conditions. It is not clear yet which view is right.

The other problem involved in many existing CHF models is that the occurrence of the burnout is always treated as a phenomenon independent of the nucleate boiling process immediately preceding it. There are two reasons to describe CHF as the extension of the nucleate boiling region not the independent outcome. Firstly, as discussed by Sadasivan *et al.* [5], all variables affecting nucleate boiling influence the transition boiling region as well. Secondly, the occurrence of dry areas at nucleate boiling region near CHF has been observed by several investigators. In fact, it is important to note that the dry region has much poorer heat transfer than the surface covered with liquid. As a result, it is reasonable to see that the boiling phenomena involved in nucleate boiling region extend to CHF.

Based on the situations discussed above, a new model to describe the phenomena of CHF is required, and the model should be consistent with observed boiling mechanisms and explain the influences of hydrodynamic conditions as well as the influences of surface conditions on CHF. Also the model would be one that is a natural outcome of the description of the high heat flux nucleate boiling region.

† Author to whom correspondence should be addressed.

NOMENCLATURE

A	shell area [m^2]
C	constant in equation (1)
CHF	critical heat flux
d	bubble diameter [m]
d_{av}	time-averaged bubble diameter [m]
d_c	cavity mouth diameter [m]
d_{max}	bubble diameter at departure [m]
h_{fg}	latent heat of vaporization [J kg^{-1}]
L	center to center distance between bubbles [m]
L_c	cut-off distance [m]
m	exponent in equation (1)
n	number of active nucleation sites
n_c	critical active site number
N	active nucleation site density [sites m^{-2}]
$\bar{N}$	average density of active nucleation sites [sites m^{-2}]
P	probability function defined by equation (2)
q	heat flux defined by equation (6) [W m^{-2}]
q_b	heat transferred by single bubble site [W site^{-1}]
q_{nb}	heat flux [W m^{-2}]
t	time [s]
T_{sat}	saturation temperature [K]
ΔT	wall superheat temperature [K].

Greek symbols

ρ_g	density of vapor [kg m^{-3}]
σ	surface tension [N m^{-1}]
ϕ	contact angle [degree].

In the present study, by describing the boiling phenomena observed in nucleate boiling region, a new dry-spot model is developed to predict CHF. The model can be applicable to most boiling conditions, based on the common mechanism that CHF is caused by the accumulation and coalescences of dry spots formed through dryout of the microlayer under a bubble. The validation of the model will be tested for forced convection boiling as well as for pool boiling.

2. BACKGROUND IN NUCLEATE BOILING REGION

As mentioned in the previous section, since the present model is based on boiling phenomena of the nucleate boiling region, it is necessary to review the relevant past work in the field. A distinctive feature of nucleate boiling is the generation of bubbles from preferential sites randomly located on the heating surface. Increasing surface superheat activates more nucleation sites, resulting in a rapid increase in heat flux. More densely distributed sites cause the interference with each other and result in the overlapping of the individual site. Hsu and Graham [7] have presented a summary of the earlier observations of several investigators with respect to dependence of site density on wall heat flux. The active site density can be represented as a function of wall superheat temperature or heat flux

$$N = Cq^m. \tag{1}$$

It is found that the exponent m on heat flux q generally varies between 1 and 2. The proportionality constant C and the magnitude of the exponent depend on several parameters such as surface wettability, the liquid properties and experimental conditions.

Gaertner [8] discovered that the bubble sites on a boiling surface are randomly distributed and can be represented by Poisson distribution. Thus the probability that NA active sites will be found in a shell area A can be calculated according to

$$P(NA) = \frac{e^{-\bar{N}A}(\bar{N}A)^{NA}}{(NA)!}. \tag{2}$$

Furthermore, Sultan and Judd [9], Del Valle and Kenning [10] and Wang and Dhir [11] reported that the distribution of local cavity population densities is described by the Poisson distribution. Kang *et al.* [12] proposed a probability model using Poisson distribution to predict the transition points on the boiling curve. Unfortunately, they did not predict the curve quantitatively.

Besides, numerous studies in the literature have focused on fluid flow in the evaporating meniscus. For example, Wayner [13] stated that the transport process depends on the intermolecular force field which is complicated function of temperature and pressure near liquid–vapor interfaces. Schonberg *et al.* [14] investigated the heat transport of a steady heptane meniscus and found that a stable evaporating meniscus with a very high heat flux (1.3–1.6×10^6 W m^{-2}) in the 2 μm microchannel was theoretically possible. Lay and Dhir [15] studied the liquid flow and heat transfer in an evaporating two-dimensional vapor stem to predict nucleate boiling heat fluxes.

The dry spots on the heating surface yield much poorer heat transfer coefficients which are same as those in film boiling. The occurrence of the dry areas was believed to be the reason causing a change in slope of the nucleate boiling curve by Gaertner and Westwater [16]. Kirby and Westwater [17], and Van

Ouwerkerk [18], conducted pool boiling on a horizontal glass surface plated with an extremely thin conducting material. They observed that the dry spots sometimes grew in size and neighboring ones would merge. Near CHF, the dry spots were frequently generated and the coalescences of dry spots were also common, and Kirby *et al.* showed that the average diameter of a dry spot, before they grew to large dry patches, was about 0.25 mm which size was almost the same as the maximum diameter of a bubble. Carne [19] studied pool boiling of organic fluids and water at atmospheric pressures on horizontal steel elements with various diameters. He observed that a small vapor patch instantaneously appeared at some random location on the heater. Katto and Yokoya [20] studied pool boiling of water at atmospheric pressure on the horizontal copper disk and observed several dry areas as well as many dry spots on the heated surface at a heat flux close to CHF. Fiori and Bergles [21] conducted photographic and electric probe studies on the CHF of subcooled flow boiling for water and proposed a CHF model based on the formation of a dry spot underneath a vapor clot. Galloway and Mudawar [22] carried out microscopic and macroscopic observations of the near-wall region for the flow boiling of dielectric fluorocarbon FC-87 at 1.37 atm and observed that a large part of heater surface was already dryout at 95% of CHF. Although the appearance of such a small and large dry spot has been observed by several researchers, it has not received much attention, and the mechanism of the formation of dry spots and their interrelation with CHF are unknown yet.

3. A DRY-SPOT MODEL FOR BOILING HEAT TRANSFER

3.1. *New concept for dry spot formation mechanism*

Gaertner [23] hypothesized that the stems of the vapor mushrooms become hydrodynamically unstable in the local surface areas which have certain critical active site population. Haramura and Katto [2] proposed a macrolayer dryout model based on Gaertner's hypothesis. Unal *et al.* [24] and Sadasivan *et al.* [5] presumed that the formation of the dry areas is a result of the evaporation of the thinner region of the local liquid macrolayer in the macrolayer dryout model. However, it is difficult to explain clearly the dry spot size observed by Kirby *et al.* [17] and the distribution by Carne [19]. It is reasonable to consider that the small dry spots were formed under bubbles and that there is a mechanism to prevent fluid flow in the evaporating meniscus discussed in the previous section.

In the present work, it is hypothesized that when the number of bubbles surrounding one bubble exceeds a critical number, the surrounding bubbles restrict the feed of liquid to the thin liquid film (microlayer) under the bubble. Then an insulating dry spot of vapor will form on the heated surface. As the surface temperature is raised, because of a dramatic increase in active nucleation site density with a small increase in wall superheat temperature, more and more bubbles will have a population of surrounding active sites over critical number. Consequently, the number of the spots will increase and the size of dry areas will increase due to merger of several dry spots. If this trend continues, the number of effective sites for heat transport through the wall will diminish and CHF occurs.

3.2. *Basic assumptions*

To simplify the modeling of the CHF phenomena, it is necessary to give out the following basic assumptions:

(1) Time-averaged bubble diameter d_{av} is representative of the diameter of bubbles, since there are coexisting bubbles of all ages, and the statistical variations in bubble departure diameter and frequency are ignored.
(2) The distribution of active nucleation sites obeys the Poisson distribution law, equation (2), and the diameter of cell is taken as twice that of the bubble. If a bubble is activated within the cell, the bubble overlaps with a bubble located at the center of the cell (see Fig. 1).
(3) The heater surface temperature does not vary temporally and spatially.
(4) The effect of overlap between bubbles on heat transfer is not large and can be ignored. Kenning and Del Valle [25] showed that the interference between bubbles has little effect on the heat transfer in fully-developed nucleate boiling.

3.3. *Proposed model*

The proposed model used here can be easily extended to transition boiling region. However, the analysis is restricted within nucleate boiling region because of the lack of some boiling parameters at high wall superheat temperature. In literature, three heat transfer modes contribute to the overall heat transfer namely: pure natural convection, pure nucleate boil-

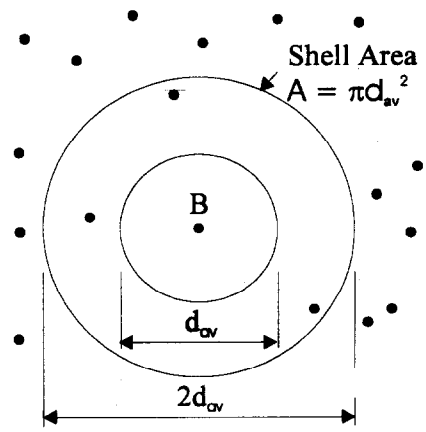

Fig. 1. Random array of active sites.

ing and pure film boiling. Pure natural convection occurs when sensible energy is removed from non-nucleating portions of the heated surface. In pure nucleate boiling, heat is removed from the heated surface by bubble activity. Pure film boiling occurs over a dry region on heating surface. For the high heat flux nucleate boiling up to CHF, it is generally known that the heat flux fractions due to pure natural convection and due to pure film boiling are much smaller than that due to pure nucleate boiling.

Let us consider the random array of active sites shown in Fig. 1. If an arbitrarily selected active site B is chosen as the center of a circle having a radius d_{av}, the probability that no active site will be found in this circle other than the selected site, which is located at the center (probability equals 1), is given by Poisson equation, equation (2):

$$P(0) = e^{-\bar{N}A}. \tag{3}$$

Similarly, the probability that n active sites will be found in a shell area A other than the selected site is

$$P(n) = \frac{e^{-\bar{N}A}(\bar{N}A)^n}{n!}. \tag{4}$$

Then the probability that the number of active site is greater than or equal to the critical active site number n_c will be found in a shell area A is

$$P(n \geqslant n_c) = 1 - \sum_{n=0}^{n_c-1} P(n). \tag{5}$$

Therefore, the heat flux contributing to nucleate boiling is obtained as the following equation:

$$q = q_b \bar{N}(1 - P(n \geqslant n_c)) \tag{6}$$

where q_b is heat transferred by single bubble site assuming each bubble site has uniform heat duty. The heat flux $q_b\bar{N}$ means physically the quantity of heat transfer of all bubbles activated without dry spot formation. If one ignores the heat flux fractions due to single phase convective heat flux and due to film boiling, the heat flux from equation (6) can be presumed as overall heat flux. To calculate the heat q_b, let us consider a typical smooth boiling curve as shown in Fig. 2. At the DNB (departure from nucleate boiling)

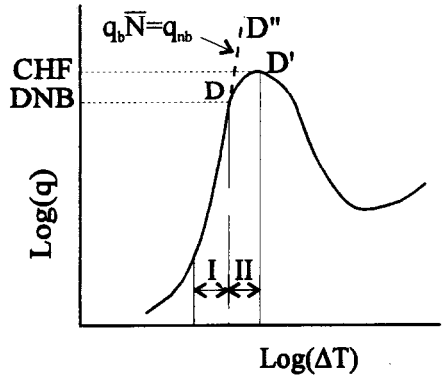

Fig. 2. Typical boiling curve.

point, the slope of boiling curve change due to appearance of dry area as discussed in the previous section. In region I, $q_b\bar{N}$ is approximately equal to q_{nb} assuming that dry area fractions on heated surface is negligible where q_{nb} is the heat flux fitting the nucleate boiling data as a function of ΔT. Also we can expect that if there was no generation of dry area in region II, heat flux increases along dotted line DD'', the extension of q_{nb}, instead of curve DD' with an increase in ΔT. Therefore, $q_b\bar{N}$ is equal to the extension of q_{nb} and then q_b is given by

$$q_b = \frac{q_{nb}}{\bar{N}}. \tag{7}$$

4. RESULTS AND DISCUSSION

To compare with experimental data, we need the information of boiling parameters measured from given experimental conditions, such as active nucleation site density, bubble departure diameter, and bubble growth rate. There are a few number of experimental data set including such boiling parameters, because many CHF studies concentrated on the measurement of CHF alone, without considering the nucleate boiling region.

The developed model is compared with the data from Dhir and Liaw [26] (see also Liaw [27]), Paul and Abdel-Khalik [28] and Del Valle and Kenning [10]. All of the experiments were performed for atmospheric boiling of water. Table 1 summarizes the conditions of the experiments. It is well known that each parameter listed in Table 1 can influence CHF. To evaluate the time-averaged bubble diameter from the measured bubble departure diameter, it is assumed that the bubble diameter varies with times as $t^{1/2}$ [29].

4.1. *The determination of critical site number and comparison with pool boiling data*

Dhir and Liaw [26] conducted experiments on the pool boiling of saturated water at 1 atm on a vertical rectangular copper surface with several contact angles. They measured time- and space-averaged wall void fraction by means of a γ-beam traversing parallel to the heated surface. To use their data in this study, we further need information on active site density and time-averaged bubble diameter. Wang and Dhir's correlation [11] was used for the active site density. They correlated their data for active nucleation site density as a function of the wall superheat and contact angle as follows:

$$\bar{N} = 5 \times 10^{-27}(1 - \cos\phi)/d_c^6 \tag{8}$$

where the cavity mouth diameter d_c is a function of the local superheating

$$d_c = \frac{4\sigma T_{sat}}{\rho_g h_{fg} \Delta T}. \tag{9}$$

To obtain the time-averaged bubble diameters with

Table 1. Experimental conditions for the data used in model validation

Reference	Flow mode	Bulk fluid temperature	Heating method	Heater geometry	Heater size	Surface wettability
Dhir and Liaw [26]	pool	saturated	indirect heating	vertical plate	63 × 103 (mm^2)	several contact angles
Paul and Abdel-Khalik [28]	pool	saturated	direct heating	horizontal wire	0.3 (mm) dia.	—
Del Valle and Kenning [10]	flow	subcooled (84 K)	direct heating	vertical plate	150 × 10 (mm^2)	—

contact angles, first, the wall void fractions were predicted from presumed time-averaged bubble diameters using the Poisson distribution of active site density and analyzing the geometry of the overlapping area between bubbles, and then it is obtained by requiring that the predicted wall void fraction as a function of heat fluxes shows good agreement with experimental data. Figure 3 shows a comparison of the predicted wall void fractions with experiments on a wall void fraction and heat flux coordinate system. The predictions are seen to compare well with the data.

Before evaluating CHF, the determination of critical site number which prevents the liquid supply to the microlayer formed under the bubble is required. In this study, it is determined by comparing with experiment data of boiling curve. Dhir and Liaw's data [26] were used for this purpose and equation (6) was simulated by assuming critical site number ($n_c = 4$, 5 and 6). Figure 4(a)–(c) show the comparison of predictions using a given critical site number as variable and measurement data from Dhir and Liaw [26] for several contact angles. Surprisingly, the predictions by equation (6) show smooth transition of boiling curve before and after CHF independent of

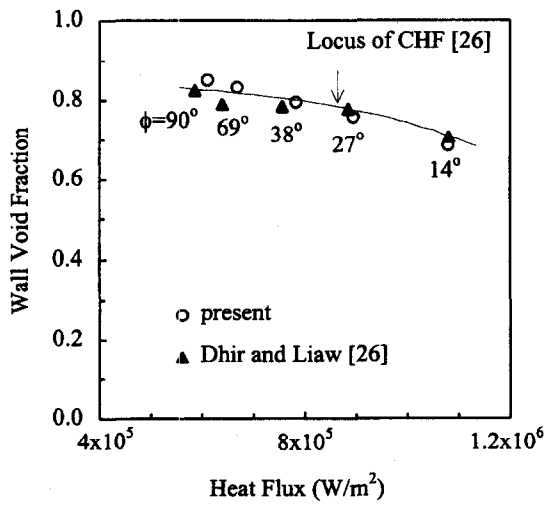

Fig. 3. Dependence of wall void fraction on heat flux.

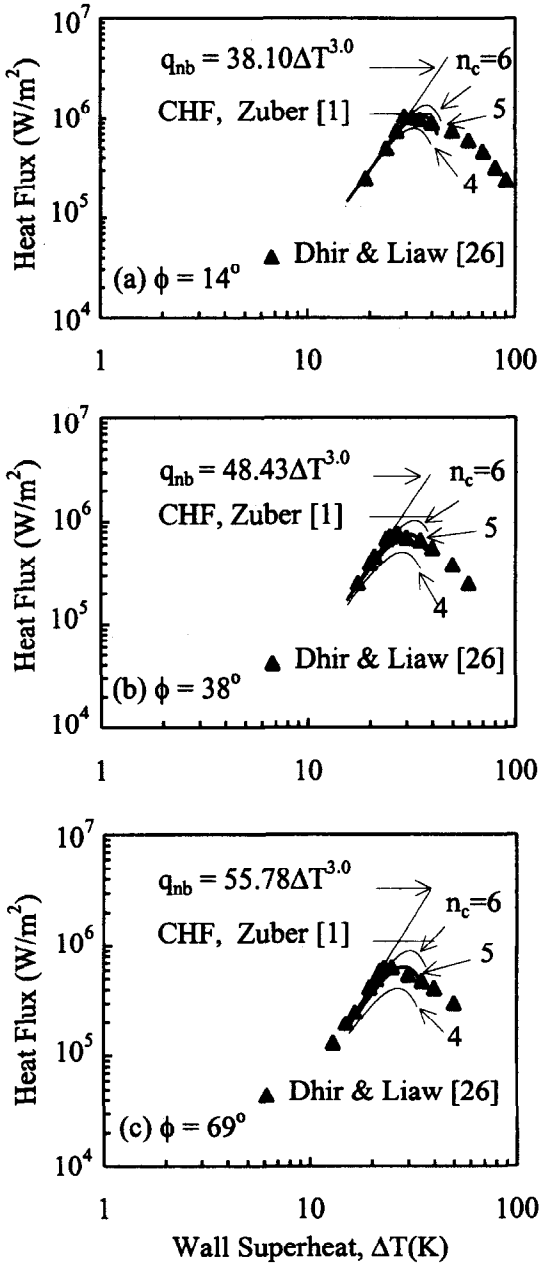

Fig. 4. Comparison of predictions by assuming critical site number and experimental data for several contact angles.

the critical site numbers. The mechanism involved is a decrease in the number of effective active sites and an increase in the number of dry spots. Also the comparison indicates that when critical site number is five, the model predictions have good agreement with measurements. It is concluded that the critical site number is five.

Figure 5(a), (b) show the different configurations of bubbles according to the number of surrounding bubbles. L_4 and L_5 represent the center to center distance of the bubbles when the numbers of surrounding bubbles are 4 and 5, respectively. L_4 is larger than L_5 because the cutoff distance L_c is inversely proportional to square root of active site number in shell area A [11]. When the number of surrounding bubbles is four as shown in Fig. 5(a), the bubble located at the center is open to bulk liquid, and then the bulk liquid can be supplied to the microlayer under bubble located at center continuously. However, when the number of surrounding bubbles is five as shown in Fig. 5(b), the bubble located at the center is isolated from the bulk liquid by the surrounding bubbles. Then it is postulated that the bulk liquid cannot be supplied to the microlayer under the bubble located at center. In this case, the microlayer can dry out, and a dry spot forms under the bubble. The bubble loses its identity as bubble and cannot transfer heat effectively.

In Fig. 6, the predicted critical heat fluxes are compared with the data obtained on several partially wetted surfaces. The predicted values are found to be in good agreement with Dhir and Liaw's data [26] for all contact angles. As shown in Fig. 6, the surface wettability plays no significant role in Zuber's model [1] for large contact angles more than 27°. The present model shows clearly the mechanism how the contact angle influences CHF. As we know, the active nucleation density and bubble departure diameter are affected by the contact angle. Also, the product of these two parameters, NA, is affected by the contact angle, and then the variation of the product induces the variation of CHF.

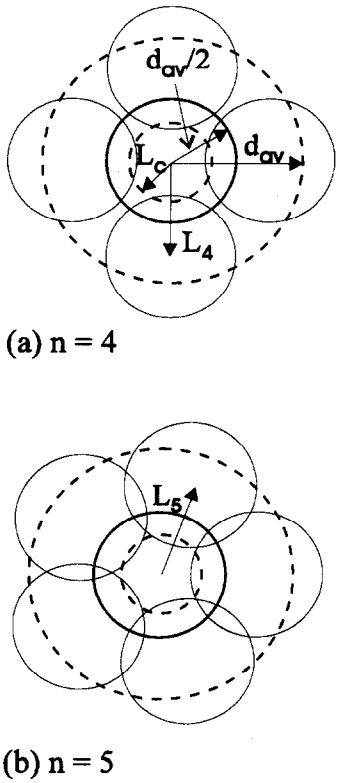

Fig. 5. Configurations of the bubbles surrounding a bubble located at center.

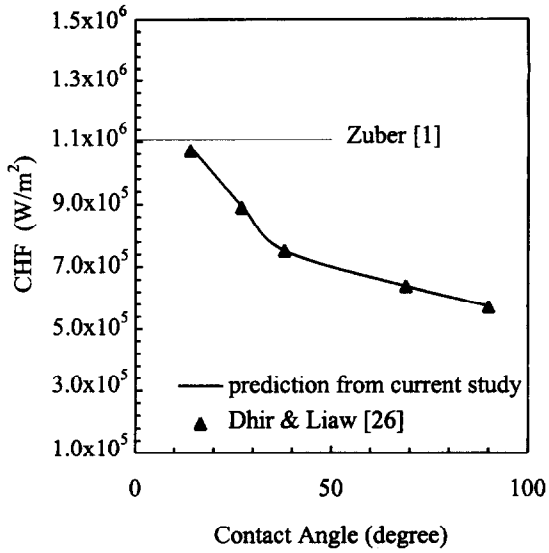

Fig. 6. Effect of surface wettability on CHF.

Paul and Abdel-Khalik [28] conducted experiments on the pool boiling of saturated water at 1 atm along an electrically heated horizontal platinum wire. Using high-speed photography, they measured active nucleation site density and bubble departure diameter up to 70% of CHF. They found that the mean number density of active nucleation sites and the average bubble departure diameter can be represented by the linear relationship with the boiling heat flux as follows:

$$\bar{N} = 1.207 \times 10^{-3} q_{nb} + 15.74 \quad (10)$$

$$d_{max} = 0.3874 \times 10^{-9} q_{nb} + 1.108 \times 10^{-3}. \quad (11)$$

Note that $\bar{N}$ in equation (10) is the average number of active nucleate sites per unit length.

The measured CHF was 0.72×10^6 W m^{-2} and the predicted value is 0.66×10^6 W m^{-2} as shown in Fig. 7. The discrepancy between the experimental CHF and predicted CHF is about 8.1%. The predictions are seen to compare well with the data.

4.2. *Comparison with flow boiling data*

Del Valle and Kenning [10] conducted experiments on the subcooled flow boiling at 1 atm. The test surfaces were stainless-steel plate heated by direct electrical current over an area 150×10 mm^2 set into one

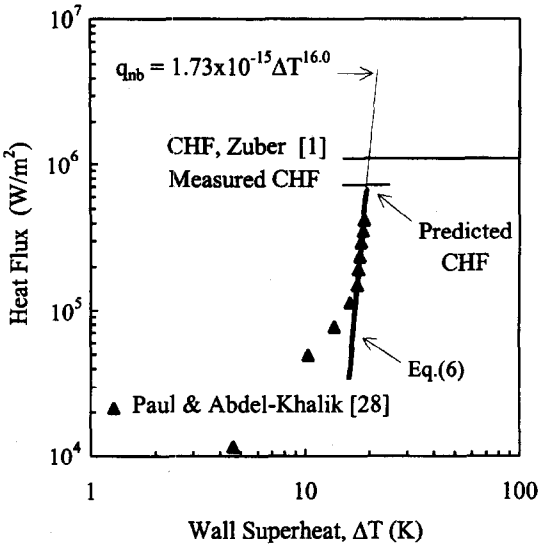

Fig. 7. Comparison of predictions with data for horizontal wire.

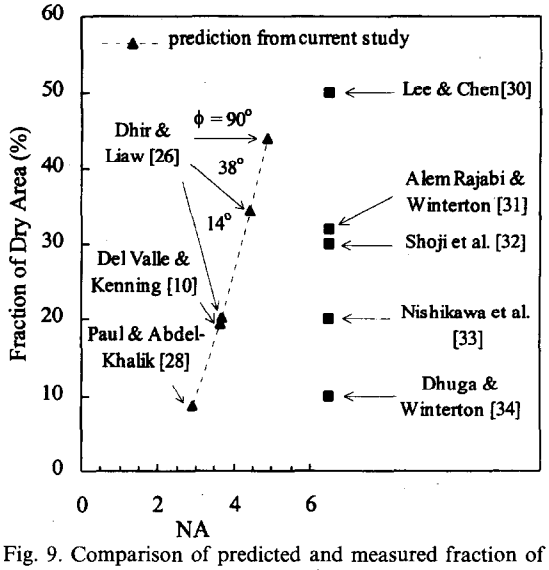

Fig. 9. Comparison of predicted and measured fraction of dry area near CHF.

side of a vertical flow channel of rectangular cross section 12×5 mm^2. They measured active nucleation site density and bubble departure diameter at heat fluxes 70, 80, 90 and 95% of CHF when the inlet velocity is 1.7 m s^{-1} and subcooling temperature 87 K. The mean maximum bubble diameter was 0.4 mm $\pm$ 5% independent of heat flux. The reported data for active nucleation site density show good linearity as a function of heat flux and can be correlated by the expression

$$\bar{N} = 2.30 q_{nb} + 10^6. \quad (12)$$

The measured CHF was 4.92×10^6 W m^{-2} and the predicted CHF by the present model is 4.65×10^6 W m^{-2} as shown in Fig. 8. The discrepancy between the experimental CHF and predicted CHF is about 5.5%.

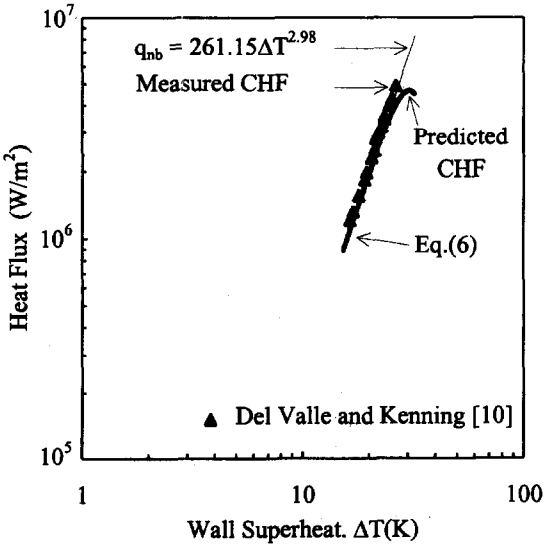

Fig. 8. Comparison of predictions with data for subcooled flow boiling.

The model predictions are quite satisfactory. Particularly, in this experiment, they observed that all runs at 84 K subcooling remained in the bubbly flow regime up to burnout (they run for several inlet velocities) and no large vapor mass. Large vapor mass is a major controlling factor for the CHF in macrolayer dryout model [2].

4.3. *The fraction of dry area*

The estimated fraction of dry area from current studies for the data used in the validation of the present model is presented in Fig. 9. The figure also shows a comparison with the measured fraction of dry area by several investigators [30–34]. The measured data spread in the range of about 10–50% and the reason of such a great spread of the data are unknown yet. It is interesting to note that the estimated fraction of dry area at CHF are not constant, but varying with data to data, i.e. depends on boiling conditions. Also the figure shows that the fraction of dry area strongly depends on NA. i.e. the higher wall void fraction at CHF, the higher the fraction of dry area.

5. SUMMARY AND CONCLUSIONS

(1) It is postulated that a dry spot is formed when the number of bubbles surrounding one bubble exceed the critical number and, as a result, the surrounding bubbles restricts the feed of liquid to the thin liquid film (microlayer) under the bubble located at center. As both the number and size of the dry spots will increase with an increase in the wall superheat temperature, the number of effective nucleation sites will diminish, and wall heat flux reaches a maximum called CHF.

(2) Based on the physical structure mentioned above, a dry-spot model has been developed. The model has been validated with existing data in pool and

flow boiling. The CHF predicted from the model compare well with existing CHF data.

(3) By means of the model, the parametric effects of flow modes and surface wettability can be reasonably explained.

(4) If the information on the active site density and bubble diameter in the nucleate boiling region is known, CHF can be determined. The active nucleation site density and bubble diameter contribute to CHF significantly.

(5) CHF must be viewed as the extension of the nucleate boiling in contrast to the traditional view of CHF as independent phenomena distinct from the nucleate boiling.

(6) A single CHF model were applied to quite different boiling conditions without any correction. It strongly supports that the basic mechanism of the CHF is same even though the boiling conditions are different.

(7) In this paper, to validate the present model, the measured information on active nucleate site density and bubble departure diameter were used. Further work on them will be required to use the present model as a prediction tool.

REFERENCES

1. Zuber, N., Stability of boiling heat transfer. *ASME Journal of Heat Transfer*, 1958, **80**, 711–720.
2. Haramura, Y. and Katto, Y., A new hydrodynamic model of critical heat flux, applicable widely to boiling to both pool and forced convection boiling on submerged bodies in saturated liquid. *International Journal of Heat and Mass Transfer*, 1983, **26**(3), 389–399.
3. Lienhard, J. H., Things we don't know about boiling heat transfer: 1988. *International Communication of Heat and Mass Transfer*, 1988, **15**, 401–428.
4. Katto, Y., Critical heat flux in pool boiling. In *Pool and External Flow Boiling*, ed. V. K. Dhir, and A. E. Bergles. ASME, New York, 1992, pp. 151–164.
5. Sadasivan, P., Unal, C. and Nelson, R., Perspective: issues in CHF modeling—the need for new experiments. *ASME Journal of Heat Transfer*, 1995, **117**, 558–567.
6. Dhir, V. K., Some observations from maximum heat flux data obtained on surfaces having different degrees of wettability. In *Pool and External Flow Boiling*, ed. V. K. Dhir and A. E. Bergles. ASME, New York, 1992, pp. 185–192.
7. Hsu, Y. Y. and Graham, R. W., *Transport Processes in Boiling and Two-Phase Systems*. Mcgraw-Hill, New York, 1976.
8. Gaertner, R. F., Distribution of active sites in the nucleate boiling of liquids. *Chemical Engineering Progress Symposium Series*, 1963, **59**(41), 52–61.
9. Sultan, M. and Judd, R. L., Spatial distribution of active sites and bubble flux density. *ASME Journal of Heat Transfer*, 1978, **100**, 56–62.
10. Del Valle, M., V. H. and Kenning, D. B. R., Subcooled flow boiling at high heat flux. *International Journal of Heat and Mass Transfer*, 1985, **28**(10), 1907–1920.
11. Wang, C. H. and Dhir, V. K., Effect of surface wettability on active nucleation site density during pool boiling of water on a vertical surface. *ASME Journal of Heat Transfer*, 1993, **115**, 659–669.
12. Kang, S., Bartsch, G., Jia, D. and Chen, X.-J., Probability model to describe pool boiling phenomena. *Proceedings of the Tenth International Heat Transfer Conference*, Brighton, U.K., 1994, Vol. 5, pp. 93–98.
13. Wayner, Jr, P. C., Intermolecular and surface forces with applications in change-of-phase heat transfer. In *Boiling Heat Transfer*, ed. R. T. Lahey, Jr. Elsevier Science Publishers, New York, 1992, pp. 569–614.
14. Schonberg, J. A., Dasgupta, S. and Wayner, P. C., Jr, An augmented young-Laplace model of an evaporating meniscus in a microchannel with high heat flux. *Experimental Thermal and Fluid Science*, 1995, **10**, 163–170.
15. Lay, J. H. and Dhir, V. K., Shape of a vapor stem during nucleate boiling of saturated liquids. *ASME Journal of Heat Transfer*, 1995, **117**, 394–401.
16. Gaertner, R. F. and Westwater, J. W., Population of active sites in nucleate boiling heat transfer. *Chemical Engineering Progress Symposium Series*, 1960, **56**(30), 39–48.
17. Kirby, D. B. and Westwater, J. W., Bubble and vapor behavior on a heated horizontal plate during pool boiling near burnout. *Chemical Engineering Progress Symposium Series*, 1965, **61**(57), 238–248.
18. Van Ouwerkerk, H. J., Burnout in pool boiling the stability of boiling mechanisms. *International Journal of Heat and Mass Transfer*, 1972, **15**, 25–34.
19. Carne, M., Some effects of test section geometry in saturated pool boiling on the critical heat flux for some organic liquids and liquid mixtures. *Chemical Engineering Progress Symposium Series*, 1965, **61**(59), 281–289.
20. Katto, Y. and Yokoya, S., Principal mechanism of boiling crisis in pool boiling. *International Journal of Heat and Mass Transfer*, 1968, **11**, 993–1002.
21. Fiori, M. P. and Bergles, A. F., Model of critical heat flux in subcooled flow boiling. *Proceedings of the Fourth International Heat Transfer Conference*, Versailles, 1970, Vol. 9, Paper B.6.3.
22. Galloway, J. E. and Mudawar, I., CHF mechanism in flow boiling from a short heated wall-I. examination of near-wall conditions with the aid of photomicrography and high-speed video imaging. *International Journal of Heat and Mass Transfer*, 1993, **36**(10), 2511–2526.
23. Gaertner, R. F., Photographic study of nucleate pool boiling on a horizontal surface. *ASME Journal of Heat Transfer*, 1965, **87**, 17–29.
24. Unal, C., Daw, V. and Nelson, R. A., Unifying the controlling mechanisms for the critical heat flux and quenching: the ability of liquid to contact the hot surface. *ASME Journal of Heat Transfer*, 1992, **114**, 972–982.
25. Kenning, D. B. R. and Del Valle, M., V. H., Fully-developed nucleate boiling: overlap of areas of influence and interference between bubble sites. *International Journal of Heat and Mass Transfer*, 1981, **24**(6), 1025–1032.
26. Dhir, V. K. and Liaw, S. P., Framework for a unified model for nucleate and transition pool boiling. *ASME Journal of Heat Transfer*, 1989, **111**, 739–746.
27. Liaw, S.-P., Experimental and analytical study of nucleate and transition boiling on vertical surfaces. Ph.D. dissertation, University of California, Los Angles, CA, 1988.
28. Paul, D. D. and Abdel-Khalik, S. I., A statistical analysis of saturated nucleate boiling along a heated wire. *International Journal of Heat and Mass Transfer*, 1983, **26**(4), 509–519.
29. Han, C. Y. and Griffith, P., The mechanism of heat transfer in nucleate pool boiling—part I, bubble initiation, growth and departure. *International Journal of Heat and Mass Transfer*, 1965, **8**, 887–904.
30. Lee, L. Y. W., Chen, J. C. and Nelson, R. A., Liquid–solid contact measurements using a surface thermocouple temperature probe in atmospheric pool boiling water. *International Journal of Heat and Mass Transfer*, 1985, **28**(8), 1415–1423.

31. Alem Rajabi, A. A. and Winterton, R. H. S., Liquid–solid contact in steady-state transition pool boiling. *International Journal of Heat and Fluid Flow*, 1988, **9**(2), 215–219.
32. Shoji, M., Witte, L. C., Yokoya, S. and Ohshima, M., Liquid–solid contact and effects of surface roughness and wettability in film and transition boiling on a horizontal large surface. *Proceedings of the Ninth International Heat Transfer Conference*, Jerusalem, Israel, 1990, Vol. 2, pp. 135–140.
33. Nishikawa, K., Fujii, T. and Honda, H., Experimental study on the mechanism of transition heat transfer. *Bulletin of JSME*, 1972, **15**, 93–103.
34. Dhuga, D. S. and Winterton, R. H. S., Measurement of surface contact in transition boiling. *International Journal of Heat and Mass Transfer*, 1985, **28**(10), 1869–1880.